Atmos. Chem. Phys. Discuss., 12, 31153–31186, 2012
www.atmos-chem-phys-discuss.net/12/31153/2012/
doi:10.5194/acpd-12-31153-2012

Atmospheric Chemistry and Physics Discussions

Comparison between summertime and wintertime Arctic Ocean primary marine aerosol properties

J. Zábori[1], R. Krejci[1,2], J. Ström[1], P. Vaattovaara[3], A. M. L. Ekman[4,5], E. M. Mårtensson[1,6], and E. D. Nilsson[1]

[1]Department of Applied Environmental Science, Stockholm University, 114 18 Stockholm, Sweden
[2]Department of Physics, University of Helsinki, 00014 Helsinki, Finland
[3]Department of Applied Physics, University of Eastern Finland, 70211 Kuopio, Finland
[4]Department of Meteorology, Stockholm University, 114 18 Stockholm, Sweden
[5]Bert Bolin Centre for Climate Research, Stockholm University, 114 18 Stockholm, Sweden
[6]Department of Earth Sciences, Uppsala University, 752 36 Uppsala, Sweden

Received: 15 November 2012 – Accepted: 23 November 2012 – Published: 5 December 2012

Correspondence to: J. Zábori (julia.zabori@itm.su.se)

Published by Copernicus Publications on behalf of the European Geosciences Union.

Abstract

Primary marine aerosols (PMA) are an important source of cloud condensation nuclei, and one of the key elements of the remote marine radiative budget. Changes occurring in the rapidly warming Arctic, most importantly the decreasing sea ice extent will alter PMA production and hence the Arctic climate through a set of feedback processes. In light of this, laboratory experiments with Arctic Ocean water during both Arctic winter and summer were conducted and focused on PMA emissions as a function of season and water properties. Total particle number concentrations and particle number size distributions were used to characterize the PMA population. A comprehensive data set from the Arctic summer and winter showed a decrease in PMA concentrations for the covered water temperature (T_w) range between −1 °C and 15 °C. A sharp decrease in PMA emissions for a T_w increase from −1 °C to 4 °C was followed by a lower rate of change in PMA emissions for T_w up to about 6 °C. Near constant number concentrations for water temperatures between 6 °C to 10 °C and higher were recorded. Even though the total particle number concentrations changes for overlapping T_w ranges were consistent between the summer and winter measurements, the distribution of particle number concentrations among the different sizes varied between the seasons. Median particle number concentrations for $D_p < 0.125$ µm measured during winter conditions were similar (deviation of up to 3 %), or lower (up to 70 %) than the ones measured during summer conditions (for the same water temperature range). For $D_p > 0.125$ µm, the particle number concentrations during winter were mostly higher than in summer (up to 50 %). The normalized particle number size distribution as a function of water temperature was examined for both winter and summer measurements. An increase in T_w from −1 °C to 10 °C during winter measurements showed a decrease in the peak of relative particle number concentration at about D_p of 0.180 µm, while an increase was observed for particles with $D_p > 1$ µm. Summer measurements exhibited a relative shift to smaller particle sizes for an increase of T_w in the range 7–11 °C. The differences in the shape of the number size distributions between winter and

ACPD
12, 31153–31186, 2012

summer may be caused by different production of organic material in water, different local processes modifying the water masses within the fjord (like sea ice production in winter and increased glacial melt water inflow during summer) and different origin of the dominant sea water mass. Further research is needed regarding the contribution of these factors to the PMA production.

1 Introduction

In recent decades environmental conditions in the Arctic region have changed rapidly, in particular in the Arctic Ocean. Changes in the Arctic Ocean sea ice and Arctic Ocean water properties are manifold: decrease of the sea ice extent, decrease of the perennial sea ice, increase of fresh water inflow, increase of water temperature, change of biological state (Parkinson and Cavalieri, 2008; Comiso et al., 2008; Johannessen et al., 1999; Nuth et al., 2010; Steele et al., 2008; Polyakov et al., 2007; Zhang, 2005; Tremblay et al., 2011). The decrease of sea ice extent should result in an increase of the sea spray source area and thereby also in an increase of the sea spray emissions.

Nevertheless, there is not much known about the effects on sea spray emissions from changes in the physical properties of sea water in the Arctic Ocean region. A number of studies have examined the influence of water temperature, salinity, and oxygen saturation on particle number characteristics using artificial sea water, Baltic Sea water and North Atlantic sea water (Mårtensson et al., 2003; Russell and Singh, 2006; Tyree et al., 2007; Hultin et al., 2011, 2010). However, a comparison between the different studies is not straightforward due to different experimental setups and water origins. Zábori et al. (2012) is, to our knowledge, the only systematic study so far combining physical properties of Arctic Ocean water (water temperature, salinity, oxygen saturation) with marine aerosol characteristics. One main finding of the Zábori et al. (2012) study was that the marine particle number concentration decreased by at least four times with an increase in water temperature from −1 °C to about 6 °C. For higher water temperatures (upper measurement limit was 9 °C), the particle number concentration

ACPD
12, 31153–31186, 2012

remained relatively constant. In this study we will examine if the trend found by Zábori et al. (2012) is consistent with measurements conducted using Arctic Ocean water at higher water temperatures, sampled during summertime, despite an expected higher biological activity during the polar day period (Hodal et al., 2012). To this end, the dependency of the total particle number concentration and number size distribution on the water temperature, for the same temperature range, is compared for summer- and wintertime measurements. In addition, the dependency of the shape of the number size distribution on water temperature is examined for the different seasons.

2 Experiments

2.1 Experimental site

Laboratory experiments using Arctic Ocean sea water were carried out at Ny-Ålesund (78°55′ N, 11°56′ E), Western Svalbard (Fig. 1a) in a marine laboratory during late Arctic summer conditions (from the 24 August to the 7 September 2009) and late Arctic winter conditions (from the 15 February to the 7 March 2010; cf., Zábori et al., 2012). Sampling locations were selected to account for outer and inner fjord conditions, where the latter was influenced by glacial melt water (Fig. 1b). During summertime, water outside the fjord mouth was sampled by boat, while the sampling took place from the coastline at the north-west side of the peninsula during winter conditions. In the inner part of Kongsfjorden, close to the glacier, water was sampled by boat during both seasons. In the laboratory, a deep water inlet is permanently installed. Thus, experiments with deep fjord water were also conducted during both campaigns. The deep water was pumped through an inline filter with a pore size of 100 µm and 20 µm from a depth of 80 m and entered the lab after being treated with UV light. The mechanical filter and UV-filter could not be bypassed. However, since the systems were not changed during the duration of the experiments, the potential effects of the filtration systems are assumed to be similar. In summer, water was additionally collected by boat north

ACPD
12, 31153–31186, 2012

of Ny-Ålesund in the middle of the fjord (Fig. 1b). The waters sampled at the different locations are referred to as "water types". "Corresponding water types" are for both seasons referred to as (a) waters sampled outside the fjord mouth (b) waters close to the glacier and (c) deep water. The meteorological conditions at the experimental site for the sampling period during summer and winter are summarized in Table 1.

2.2 Factors influencing the environment within Kongsfjorden

2.2.1 External factors

In general, the atmospheric general circulation and the seasonality of available sunlight are the two external factors influencing the environment within Kongsfjorden. High pressure systems over the Arctic Ocean and Greenland as well as the Icelandic Low are the main atmospheric drivers for the weather patterns on Spitsbergen, which are generally characterized by northward advection of relatively warm and humid air from the North Atlantic (Svendsen et al., 2002).

The biology within Kongsfjorden is regulated by the availability of sunlight. The polar day period (lasting nowadays from 18 April to 23 August) is promoting the phytoplankton productivity during the summer months, while during polar night (lasting nowadays from 25 October to 17 February) the productivity is inhibited (Svendsen et al., 2002; Hop et al., 2002; Hodal et al., 2012). A spring bloom, peaking in May, has been reported to be the only predictable bloom in Kongsfjorden, while blooms during summer occur irregularly (Hodal et al., 2012; Hop et al., 2006, 2002).

2.2.2 Internal factors

Phytoplankton production within Kongsfjorden is also regulated by internal factors. Generally, high concentrations of sediments resulting from an increase of river discharge and ice melt during summer decrease the transparency of the water, especially in the inner part of the fjord, and thereby control the phytoplankton growth (Hop et al.,

ACPD
12, 31153–31186, 2012

2002; Svendsen et al., 2002). In the outer parts of the fjord the phytoplankton growth is instead limited by grazing during the summer months (Hop et al., 2002).

Two main water masses are normally flowing northwards along the west coast of Spitsbergen. The West Spitsbergen Current (WSC) transports relatively warm and saline Atlantic water ($T_w > 3$ °C, salinity > 34.9 psu) and mixes with the cooler and fresher Arctic water (−1.5 °C < T_w < 1.0 °C, 34.30 psu < salinity < 34.80 psu) on the western shelf of Spitsbergen (Piehl Harms et al., 2007; Svendsen et al., 2002). The dominance of one of these water masses changes during the year. During autumn and winter, the Arctic Water mass generally dominates, while the Atlantic Water is more prevalent during summer months (Hop et al., 2006). In Kongsfjorden, the water masses are modified by inflow of fresh waters from rivers and glaciers during summer and by surface cooling and ice formation during winter (Piehl Harms et al., 2007).

The climate of the west coast of Spitsbergen is influenced by the large amount of heat which is transported northwards by the WSC. This leads to a mostly ice-free ocean along the west coast of Svalbard and to relatively mild air temperatures compared to other locations at a similar latitude. The mean air temperature at Ny-Ålesund from 1961 to 1990 was about −15 °C in February and about 4 °C in July (Svendsen et al., 2002). The average annual sea water temperature in Kongsfjorden has been estimated to be slightly above 0 °C and sea ice formation in winter is most pronounced close to the coast and in the inner parts of the fjord (Ito and Kudoh, 1997; Svendsen et al., 2002).

2.3 Experimental setup

The experimental setup was similar for summer and winter experiments. Nevertheless some differences in water flow and dilution rate by clean air occurred. Collected sea water was poured into a storage stainless steel 190 L tank situated in the laboratory. From the steel tank the water was pumped into a carefully sealed polyethylene bottle (Nalgene Labware) using an aquarium centrifugal pump (EHEIM) at a rate of 2.2 L min^{-1} during summer experiments and at a rate of 4.8 L min^{-1} during winter experiments. Different positions of the pump during different seasons caused the different pumping

ACPD
12, 31153–31186, 2012

rates. The water entered the bottle through a stainless steel nozzle with an inner diameter of 5 mm producing a water jet mimicking a wave crest, which entrains air into sea water. The air subsequently breaks up into bubbles, which burst at the water surface. The distance between the nozzle exit and the water surface was approximately 16 cm (for both the winter and summer experiments). The water level in the polyethylene (PET) bottle was kept stable by a simple overflow system and the water volume remained constant at 10 L. Water flowing from the PET bottle was transferred back to the buffer storage tank through a PVC tube (more details about the experimental procedure can be found in Sect. 2.5).

Fuentes et al. (2010a) compared different mechanisms for marine aerosol production in laboratory experiments with respect to their ability to reproduce a realistic oceanic bubble size spectrum. It was concluded that a plunging water jet was the best method for reproducing the shape of an oceanic bubble size spectra (cf., also Hultin et al., 2010). Hence, it is assumed that this method also results in the most realistic bubble-mediated aerosol size spectra (i.e. neglecting spume droplets produced from the tearing of breaking waves).

To avoid any contamination by room air, air was pumped through an ultra filter (type H cartridge, MSA, Pittsburgh) resulting in particle free air into the PET bottle. The flow rate was 9 L min^{-1} for summer experiments and 12 L min^{-1} for winter experiments, respectively. Excess air was allowed to freely leave the top of the PET bottle through an opening of 5 mm in diameter. The quality of the particle-free air and the integrity of the whole setup were regularly checked by switching off the water jet. The sample air was collected from an air volume above the sea water in the PET bottle. The total sampling air flow was kept stable at 7.2 L min^{-1} (summer) and at 5.0 L min^{-1} (winter) during all experiments. A schematic of the experimental setup is shown in Fig. 2.

2.4 Instrumentation

The air sampling from the PET bottle was conducted through a 2 m long 1/4″ stainless steel tube to the instrumental payload. Based on the geometry of the aerosol sampling

ACPD
12, 31153–31186, 2012

lines and associated inertial losses, the largest particles reliably detected were estimated to be around 5 µm in diameter (D_p). The total aerosol number concentration was measured at 1 Hz for particles with a $D_p > 0.01$ µm using a TSI model 3010 Condensation Particle Counter (CPC) and for particles with a $D_p > 0.25$ µm using a GRIMM 1.109 Optical Particle Counter (OPC).

The size distribution for the size range 0.01 µm $< D_p <$ 0.30 µm was determined using a closed-loop sheath air custom-built differential mobility particle sizer (DMPS) equipped with a TSI 3010 CPC. One scan covering 15 size bins was completed in 2.5 min. The aerosol size distribution in the range $0.25 < D_p < 32$ µm was determined every 6 s with a GRIMM 1.109 Optical Particle Counter (OPC), sizing particles in 31 bins. The relative humidity of the sampled air was monitored in the sampling line prior to entering individual instruments with a Hygroclip SC04 hygrometer (Rotronic). The relative humidity during the experiments was lower than 30 % (winter and summer). Hence, we can safely assume that the observations were representative for dry diameter aerosol particles.

Water temperature, salinity and oxygen saturation were continuously measured in the steel tank with a Stratos 2402 Cond and a Stratos 2402 Oxy from the Knick Elektronische Messgeräte GmbH & Co.

2.5 Experimental procedure and data analysis

The sampled water from the different locations (cf., Sect. 2.1) was split up in two parts to be used in two experiments for each water type (in the range from 55 L to 140 L for each individual experiment). In summer, the two experiments with the same type of water were conducted the same day, except for one case when the second sample was stored until the following day. In the winter, half of the samples were stored in a dark room at 4 °C to be used for experiments on the consecutive day. The reason for this difference in procedure was that during wintertime field sampling was more time consuming and it was not possible to conduct more than one experiment per day.

ACPD
12, 31153–31186, 2012

After the water samples were poured into the storage tank and the PET bottle, the water temperature increased due to the exposure to room temperature. Warming rates during both summer- and wintertime experiments were both on average between 1 °C h^{-1} and 2 °C h^{-1}. While water temperatures covered the range between −2 °C and 10 °C during the winter experiments, water temperatures were between 5 °C and 16 °C during the summer experiments.

The analysis strategy was: (1) based on corresponding water types, to compare the total particle number concentrations for the summer and winter data as a function of water temperature with a focus on the overlapping T_w ranges between the two seasons; (2) to compare the whole particle number size distribution (i.e. the shape and particle number concentration for different size intervals) for corresponding water types and temperature ranges for both the summer and winter data; (3) to compare separately for winter and summer data, the particle number size distribution shape for each water type and its dependency on water temperature.

The particle number concentrations were adjusted for different dilution rates of the aerosol sample by clean particle free air. That is, observed concentrations are normalized to the relative amount of particle free air introduced to the vessel compared to the sample air flow. For a comparison of the winter and summer total particle number concentration data, total particle number concentration medians were calculated for 1 °C temperature bins for each different water type.

To compare summer and winter particle number size distributions, median number size distributions were calculated for overlapping water temperature (T_w) ranges for the different water types. Median particle number size distributions were calculated for overlapping temperature ranges: 6–7 °C for deep fjord water, 5–10 °C for close to glacier water, and 6–10 °C for fjord mouth water. For all size distributions, the medians are based on total experiment measurement times ranging between about 76 min and 5 h 10 min, except for the winter size distribution outside the fjord mouth for the T_w range 7–8 °C, where the total measurement time was only 10 min.

ACPD
12, 31153–31186, 2012

To emphasize differences in the dependency of the shape of the aerosol size distributions on water temperature, each median distribution was normalized to its integral number density. The shape comparisons were made separately for summer and winter measurements, respectively. The total average measurement time for which the medians of the size distributions are based on is 2 h 13 min, with 5 min as the shortest measurement time and 6 h 52 min as the longest.

The first two OPC bins were not used in the analysis of the winter data, and subsequent calculations, but are presented for completeness. There is evidence that for the overlapping size range of the DMPS and OPC instruments, the DMPS measurements provide higher quality data. Including the first two channels of the OPC led to an overestimation of the total particle number, when integrating over the whole particle number size distribution.

3 Results

3.1 Comparison of total particle number concentrations from summer and winter measurements

Median particle number concentrations for both $D_p > 0.01\,\mu m$ and $D_p > 0.25\,\mu m$ as a function of water temperature were compared for summer and winter measurements for the three different sampling locations (Fig. 3a–c). In addition, the dependency of the resulting ratio between particles $D_p > 0.01\,\mu m$ and $D_p > 0.25\,\mu m$ on water temperature was compared for summer and winter conditions (Fig. 3d). Three patterns can be observed: (i) particle number concentrations decrease with increasing T_w up to a water temperature of about 5–7 °C (4–5 time decrease from about 1 °C to 6 °C for all different water types and $D_p > 0.01\,\mu m$) and stay relatively constant for higher water temperatures (in accordance with Zábori et al., 2012); (ii) in general, no distinct concentration shift for particles with $D_p > 0.01\,\mu m$ between the summer and winter measurements can be observed in the overlapping temperature bins; (iii) for overlapping water temperature

ACPD
12, 31153–31186, 2012

ranges, summer measurements show on average a ratio of three and winter measurements a ratio of two for particle concentrations of $D_p > 0.01\,\mu m / D_p > 0.25\,\mu m$.

Even if the dependency of particle number concentrations on water temperature is consistent for winter and summer measurements, summer particle number concentrations for $D_p > 0.01\,\mu m$ are about 2–3 times higher than the particle number concentrations recorded during winter for the lowest overlapping temperature bin (T_w between 5 °C and 6 °C). This is observed for water sampled close to the glacier and at the fjord mouth. However, it should be noted that the interquartile range is relatively large (Fig. 3b, c).

3.2 Particle number size distributions from summer and winter measurements

Particle number size distributions based on Arctic summer and Arctic winter measurements are compared for overlapping water temperature ranges for different water types (Figs. 4–6). A two-sample Kolmogorov-Smirnov test, at a 95 % confidence level, was applied to all data to test the significance of any differences between the size distributions. Additionally, the relative difference in total particle number concentrations for $D_p < 0.125\,\mu m$ and $D_p > 0.125\,\mu m$ are compared between summer and winter measurements. The division into these sizes was made as the relation between summer and winter data seem to change at about D_p 0.125 µm.

Figure 4 shows median number size distributions resulting from water sampled close to the glacier. For the lowest overlapping T_w range between 5 °C and 6 °C, significantly higher particle number concentrations for D_p from about 0.02 µm to 0.700 µm were observed for water sampled during summer conditions (Fig. 4a). For larger and smaller sizes within the T_w range of 5–6 °C the particle number concentrations do not differ significantly.

Figure 4b compares median number size distributions of summer and winter measurements for T_w between 7 °C and 8 °C. No significant differences in concentrations between the summer and winter experiments occurred for particle sizes $D_p < 0.025\,\mu m$. Up to about D_p 0.125 µm, significantly higher particle number concentrations for the

ACPD
12, 31153–31186, 2012

summertime conditions are found compared to concentrations during wintertime, although the median concentrations do not differ much (difference of about 3 %). For sizes about $D_p > 0.125\,\mu m$, winter concentrations are generally significantly higher than summer concentrations, except for the size range between D_p 0.265 and D_p 0.750 µm. Generally, particle number concentrations are comparable for winter and summer measurements for $D_p < 0.125\,\mu m$ and are about 50 % higher for the winter measurements for $D_p > 0.125\,\mu m$.

Figure 4c displays summer and winter size distributions resulting from waters having a T_w between 8 °C and 9 °C. Particle number concentrations do not differ significantly for $D_p < 0.015\,\mu m$ between summer and winter measurements. Significantly higher concentrations during summertime occur for the size range D_p 0.015–0.060 µm. Winter concentrations are generally significantly higher than summer concentrations for particles with about $D_p > 0.060\,\mu m$. Particle number concentrations are for $D_p < 0.125\,\mu m$ about 20 % higher for summer than winter measurements and for $D_p > 0.125\,\mu m$ about 40 % lower for summer compared to winter.

Figure 4d presents size distributions of both seasons resulting from 9 °C to 10 °C warm water. No significantly different particle number concentration between summer and winter measurements for the smallest particle sizes ($D_p < 0.025\,\mu m$) was detected. Up to about D_p 0.100 µm significantly higher particle number concentrations for the summertime conditions are found compared to concentrations during wintertime. Generally, particles sizes larger than D_p 0.100 µm show significantly higher winter concentrations than summer concentrations. Particle number concentrations for $D_p < 0.125\,\mu m$ are comparable for summer and winter measurements (difference of about 2 %) and for $D_p > 0.125\,\mu m$ about 50 % lower for summer compared to winter measurements.

Figure 5 compares median number size distributions of summer and winter measurements resulting from water sampled at the fjord mouth for overlapping T_w ranges. Figure 5a shows summer and winter particle number concentrations for water temperatures between 6 °C and 7 °C. Summer particle number concentrations are significantly

ACPD
12, 31153–31186, 2012

higher than winter particle number concentrations for sizes between D_p 0.015 µm and 0.223 µm. The winter particle number concentration is significantly higher for sizes between 1.450 µm to 5 µm. Particle number concentrations of the other measured sizes are not significantly different between summer and winter measurements.

Figure 5b presents median particle number concentrations of summer and winter measurements for the water temperature range 7–8 °C. Summer particle number concentrations are significantly higher for D_p 0.02–0.140 µm and for D_p 0.200–0.223 µm. The winter particle number concentrations are significantly higher than the summer particle number concentrations for D_p 0.265–0.425 µm and for D_p 0.625–5.0 µm. Particle number concentrations of the other measured sizes are not significantly different between summer and winter measurements. Particle number concentrations are for $D_p < 0.125$ µm about 70 % higher for summer than winter measurements and for $D_p > 0.125$ µm about 30 % lower for summer compared to winter.

Figure 5c displays a comparison between winter and summer particle number concentrations for water temperatures between 8 °C and 9 °C. Summer particle number concentrations are significantly higher for sizes between D_p 0.014 µm and 0.125 µm and winter particle number concentrations are higher for the size ranges D_p 0.010–0.0125 µm; D_p 0.158–0.177 µm and for 0.265–5 µm. Particle number concentrations of the other measured sizes are not significantly different between summer and winter measurements. Particle number concentrations are for $D_p < 0.125$ µm about 55 % higher for summer than winter measurements and for $D_p > 0.125$ µm about 40 % lower for summer compared to winter.

Figure 5d compares summer- and wintertime measurements of particle number size distributions for water temperatures between 9 °C and 10 °C. It is illustrated that particle number concentrations for the size range D_p 0.016–0.125 µm are significantly higher for the summer measurements compared to the winter measurements. Particle number concentrations for the size ranges between D_p 0.010–0.012 µm, between D_p 0.141–0.200 µm and between D_p 0.265–5 µm are significantly larger for winter measurements compared to summer measurements. Particle number concentrations are

ACPD
12, 31153–31186, 2012

for $D_p < 0.125\,\mu m$ about 60 % higher for summer than winter measurements, and for $D_p > 0.125\,\mu m$ about 45 % lower for summer compared to winter.

Figure 6 shows particle number size distributions based on experiments with deep water for summer- and wintertime, for the only common water temperature range of 6–7 °C. Both size distributions overlap for D_p between approximately 10 and 20 nm and for the size range D_p 0.125–0.300 µm, which is supported by the significance test. Between D_p 0.020 µm and 0.125 µm, the particle number concentration based on summer measurements exceeds significantly the one based on winter measurements, while for $D_p > 0.300\,\mu m$ the opposite result is obtained.

The normalized dependency of the particle number size distributions on water temperature are presented in Figs. 7 and 8 for summer and winter conditions, respectively. The experiments with deep sea water cover the smallest T_w range during summer measurements (6–10 °C) and result in normalized median number size distributions with similar shape for all individual T_w ranges (Fig. 7a). Experiments conducted with water sampled close to the glacier, sampled at the fjord mouth and sampled at the middle of the fjord (Fig. 7b–d) show a decrease of the relative particle density in the accumulation mode and a shift towards smaller sizes (with a local maximum at about D_p 0.05 µm) with increasing T_w from about 5–7 °C to about 10–15 °C. A different pattern is observed for the normalized particle number concentrations based on winter measurements (Fig. 8a–c). For the accumulation mode, the relative particle number concentration is indeed decreasing with increasing water temperature (from about −1–3 °C to about 6–10 °C) for a part of the size range (D_p 0.100–0.300 µm), but at the same time an increase in the relative particle number concentration for particles with $D_p > 1\,\mu m$ is observed for all water types.

4 Discussion

Despite the aim to reproduce the technical conditions of the summertime measurements during the wintertime campaign, differences in the dilution rate of the aerosol

ACPD
12, 31153–31186, 2012

samples by clean air and the water pump rate could not be avoided. Whereas data could be adjusted for the different dilution factors, it was not possible to correct for the different water flow rates. It cannot be excluded that different water flows during summer and winter experiments led to different aerosol characteristics. Fuentes et al. (2010a) examined the bubble spectra generated by a plunging-water jet system, as a function of water recirculation rate. Especially for the larger bubbles, differences for different water flow rates occurred. These larger bubbles in the water (bubble diameter > 1–2 mm) are important for the film drop production, meaning submicron aerosol production. However, a comparison of normalized particle number size distributions caused by a water pumping rate of 3 L min^{-1} and 4.8 L min^{-1} showed no appreciable differences. Nevertheless, it cannot be excluded that differences in shape do not occur when comparing particle number size distributions caused by pumping rates of 2.2 L min^{-1} (summer measurements) and 4.8 L min^{-1} (winter measurements). Despite the different water flow rates during the seasons, the results show a consistent particle number concentration for overlapping T_w ranges for the summer and winter measurements (Fig. 3a–c). This tends to support the presumption that differences in water flow rates within our experiments do not contribute significantly to the observed pattern during both seasons. Differences of up to more than 50 % between the particle number concentration of summer and winter measurement only occur for the lowest overlapping T_w range. The total measurement time was per water temperature bin rather long (more than one hour) and therefore the difference cannot be explained by natural variability of the data. Since this offset is observed during the first hours of the experiment, it is likely that the setup system was not yet stable. The relatively large interquartile range observed for the summertime lowest T_w range also supports the conclusion that the system was unstable for these measurements. Interestingly, the particles $D_p < 0.250\,\mu m$ were more affected than the particles $D_p > 0.250\,\mu m$. This indicates that the particles with $D_p < 0.250\,\mu m$ and with $D_p > 0.250\,\mu m$ are produced from different processes and the instability is only influencing the process producing particles with $D_p < 0.250\,\mu m$, which predominantly originates from film drops.

ACPD
12, 31153–31186, 2012

Although, a consistent dependency of the particle number concentration on water temperature was observed for the two seasons, there are significant differences between summer and winter particle number size distributions for the overlapping water temperature ranges (excluding Figs. 4a and 5a for which a not yet stable setup system can be assumed). For measurements based on fjord mouth water representing open sea conditions, higher particle number concentrations of particles smaller than about D_p 0.125 µm were registered in summer. However, this feature was not observed for measurements based on water sampled close to the glacier. One possible explanation is that photoautotrophic species are a source of material, likely of organic nature, which is important for formation of small sea spray particles. The availability of light is often considered to be the limiting factor for phytoplankton growth (Hop et al., 2002; Hodal et al., 2012). The waters close to the glacier are characterized by high sediment loads during summer, which weakens the penetration of sunlight into the water column inhibiting the activity of photoautotrophic species (Hop et al., 2002; Svendsen et al., 2002). Several studies showed that during phytoplankton blooms in the North Atlantic the submicron PMA is enriched with organic matter compared to the super micrometer particles (Cavalli et al., 2004; O'Dowd et al., 2004; Facchini et al., 2008). Fuentes et al. (2010b) observed an increase in the production of particles with $D_p < 100$ nm and a shift towards smaller particle sizes with an increase of a phytoplankton bioexudate concentration in a sea water proxy. If this observation is transferable to our experiments, it would result in a relatively lower small particle production from water sampled close to the glacier compared to the particle production from open sea water. Another explanation is that the water sampled close to the glacier is mostly melt water (as surface water was sampled), and therefore does not contain as much biological material as, e.g. the water sampled at the fjord mouth. This is supported by the particle number size distribution resulting from deep fjord water which resembles the size distributions from water close to the fjord mouth. Since no chemical analysis of the sampled aerosol was made in this work, we cannot prove that the organic material from the phytoplankton influenced the particle number size distribution.

ACPD
12, 31153–31186, 2012

The enhancement of the amount of smaller particles during summer forms a contrast to the observed relative increase in particle number concentrations of larger particles with an increase in T_w during winter measurements (Figs. 7 and 8). Besides biological production in summer and local effects (sea ice formation, different sediment loads), changes of water characteristics between the two seasons may also occur due to different contributions by Arctic and Atlantic waters. During the winter months, the water in Kongsfjorden is more influenced by Arctic water, while during summertime Atlantic water is dominating the water mass in the fjord. In this context, it is interesting to note that the dominance of one specific water mass during each season may change in the future due to a changing climate. However, to this point no significant change in the water volume of Atlantic water supplying the West Spitsbergen Current was observed, examining the years 1997–2010 (Beszczynska-Möller et al., 2012).

A relationship between particle number concentration and water temperature has been reported in previous studies (e.g. Mårtensson et al., 2003; Hultin et al., 2011; Bowyer et al., 1990). However, no comparison between particle number concentration and size distributions resulting from biological productive (summer conditions) and less biological productive (winter conditions) waters has, to our knowledge, been made. This study showed differences in aerosol characteristics between summer and winter measurements. However, predictions of future aerosol characteristics resulting from an increase in water temperature caused by climate change are difficult. The warming rates of about 1–2 $^{\circ}$C h^{-1} during the experiments represent more or less instantaneous temperature changes which cannot be directly compared to the slow changes expected by climate change. Long-term changes in biological and chemical processes occurring in the real Arctic Ocean are not captured by our experiments.

5 Future implication

The decrease in Arctic sea ice extent due to the climate warming, pronounced especially in the Arctic, will be followed by changes in a number of different processes, which

ACPD
12, 31153–31186, 2012

eventually will lead to different feedbacks. Figure 9 displays a potential feedback loop focused on processes related to PMA production and changes in sea ice cover, given in the light of the knowledge learned from this study. The figure serves to exemplify key pathways related to this study and not every possible feedback process related to aerosol direct and indirect effects that may be affected by climate change. For example, processes related to secondary marine aerosol production, e.g. due to changes in DMS (Charlson et al., 1987) and other volatile organic marine emissions (Vaattovaara et al., 2006; Modini et al., 2009), are not considered.

The decrease in sea ice extent should result in an increase of the primary marine aerosol source area as well as to an increase of the sea water temperature (Fig. 9). If the water temperature change takes place for $T_w >$ about 6 °C, no sea ice will be present (assuming no change of PMA due to a change in source area) and the water temperature dependency of the PMA production seems to vanish for these temperatures (cf., Sect. 3.1). In other words for water temperatures above 6 °C, a change in PMA production should be occur due to, e.g. changes in the general atmospheric circulation. Assuming a change of T_w in the lower water temperature range (below 6 °C), the net resulting change in the PMA production due to the two factors (increasing T_w and increasing source area) is currently not known (since they have opposite signs on the PMA production) and should be studied in the future, for example with the help of modeling tools. Likely, there will be a water temperature range for $T_w < 6$ °C when there is no sea ice and PMA production is effected only by the temperature dependent trend. Moreover, this picture will be modified by changes in atmospheric circulation and related wind speed over the ocean as well as by changes in marine biology of the warmer sea. Generally, the change in PMA production has important implications for the number of available cloud condensation nuclei (CCN) in the Arctic region. Our limited knowledge on how the Arctic CCN characteristics may change in a changing climate affects our ability to predict future changes in cloud cover. The supersaturation of water vapor in the atmosphere together with the availability, size, and composition of CCN determines if and where cloud droplets and clouds form. The amount of water

ACPD
12, 31153–31186, 2012

vapor in the Arctic atmosphere is dependent on the sea ice cover, the water temperature and the air temperature. Less sea ice cover and an increase in water temperature should result in an increased transport of water vapor to the atmosphere. This is so, as the sea ice represents an evaporation barrier for the water and higher water temperature increases the evaporation. As the air temperature increases it is likely that more water vapor remains in the atmosphere before condensation takes place and consequently would intensify the warming in the Arctic. The fourth parameter besides PMA source area, water temperature and water vapor that is influenced by a decreasing sea ice extent is the surface albedo, which is decreasing with a decrease in sea ice cover.

The decrease in surface albedo, together with the increase in water vapor, the unknown change in PMA production and the unknown change in cloud properties close the feedback loop and impact on the warming of the Arctic. Both the decrease in surface albedo and the increase in water vapor are expected to have a positive feedback on the warming of the Arctic. Estimates of the direct and indirect effect of aerosols, and if they will increase or decrease, is beyond the scope of this study, but our results point to an important process in the warming Arctic where PMA emission potential is strongly inversely dependent on sea water temperature. It is not possible at this point and with the presented data to assess the net sign and magnitude for all the feedbacks in the warming Arctic linked to changes of sea ice coverage and PMA production. Nevertheless, the non-linear relation between PMA production and an increase in sea water temperature, together with associated changes in sea ice cover have a strong potential to contribute to the evolution of the Arctic climate and deserve future attention.

6 Summary and conclusions

During previous laboratory experiments with Arctic Ocean water sampled during wintertime at Kongsfjorden/Western Spitsbergen, an increase of water temperatures close to the freezing point was found to give a decrease in the particle number concentration (Zábori et al., 2012). The present study aims to determine if this trend is consistent

ACPD
12, 31153–31186, 2012

with laboratory measurements conducted using Arctic Ocean water with higher water temperatures sampled during summertime, despite an expected difference in the content of organic material in water, different local processes modifying the water masses within the fjord (like sea ice production in winter and increased glacial melt water inflow during summer) and different origin of the dominant water mass between the two seasons.

To this end, measured total particle number concentrations as a function of water temperature were compared for both seasons using water sampled at the fjord mouth, close to the glacial front and from a permanent deep water inlet. In addition, particle number size distributions were compared for the overlapping water temperature ranges between summer- and wintertime. Normalized particle number size distributions as a function of water temperature were also examined over the whole water temperature range for both seasons.

Key findings are summarized below:

1. The trend in total particle number concentrations as a function of water temperature is consistent between summer and winter measurements.

2. Particle number concentrations decrease by 4–5 times with increasing T_w from about 1 °C to 6 °C (for particles with $D_p > 0.01$ µm). For higher water temperatures, the concentrations remain relatively constant.

3. For overlapping water temperature bins, median particle number concentrations resulting from water sampled during summertime are similar or up to 70 % higher than during wintertime for particles with $D_p < 0.125$ µm. For $D_p > 0.125$ µm, the particle number concentrations during winter were mostly higher than in summer (up to 50 %).

4. During both seasons, a decrease in the relative particle number concentration for D_p 0.100–0.300 µm with increasing T_w is observed. At the same time, a relative increase of particles with $D_p > 1$ µm and $D_p < 0.100$ µm is observed for winter and summer measurements, respectively.

ACPD
12, 31153–31186, 2012

5. Changes in direct and indirect effects of primary marine aerosols may occur as a consequence of a decreasing sea ice extent. These changes are in turn likely to depend on the sea water temperature range. The sign of the feedback from a change in primary marine aerosol production may therefore be different for summer- and wintertime conditions in the Arctic.

Acknowledgements. We would like to thank the Kings Bay Marine Laboratory, Norwegian Polar Institute (NPI) staff and Kai Rosman for their support during the field experiment at Ny-Ålesund. The Norwegian Meteorological Institute is acknowledged for providing the meteorological data. This work was funded by the Swedish Research Council FORMAS and supported by the Finnish Cultural Foundation through the Lapland regional fund and by the Magnus Ehrnrooth foundation. The European Centre for Arctic Environmental Research in Ny-Ålesund (ARCFAC V) is acknowledged for support (ARCFAC-026129-2009-39), as well as the Cryosphere-atmosphere interactions in a changing Arctic climate (CRAICC) initiative and the Swedish Polar Research Secretariat for providing field equipment.

References

Beszczynska-Möller, A., Fahrbach, E., Schauer, U., and Hansen, E.: Variability in Atlantic water temperature and transport at the entrance to the Arctic Ocean, ICES J. Mar. Sci., 69, 852–863, 2012. 31169

Bowyer, P. A., Woolf, D. K., and Monahan, E. C.: Temperature dependence of the charge and aerosol production associated with a breaking wave in a whitecap simulation tank, J. Geophys. Res.-Oceans, 95, 5313–5319, doi:10.1029/JC095iC04p05313, 1990. 31169

Cavalli, F., Facchini, M. C., Decesari, S., Mircea, M., Emblico, L., Fuzzi, S., Ceburnis, D., Yoon, Y. J., O'Dowd, C. D., Putaud, J., and Dell'Acqua, A.: Advances in characterization of size-resolved organic matter in marine aerosol over the North Atlantic, J. Geophys. Res., 109, D24215, doi:10.1029/2004JD005137, 2004. 31168

Charlson, R. J., Lovelock, J. E., Andreae, M. O., and Warren, S. G.: Oceanic phytoplankton, atmospheric sulphur, cloud albedo and climate, Nature, 326, 655–661, doi:10.1038/326655a0, 1987. 31170

ACPD
12, 31153–31186, 2012

Comiso, J. C., Parkinson, C. L., Gersten, R., and Stock, L.: Accelerated decline in the Arctic sea ice cover, Geophys. Res. Lett., 35, L01703, doi:10.1029/2007GL031972, 2008. 31155

Facchini, M., Rinaldi, M., Decesari, S., Carbone, C., Finessi, E., Mircea, M., Fuzzi, S., Ceburnis, D., Flanagan, R., Nilsson, E., de Leeuw, G., Martino, M., Woeltjen, J., and O'Dowd, C.: Primary submicron marine aerosol dominated by insoluble organic colloids and aggregates, Geophys. Res. Lett., 35, L17814, doi:10.1029/2008GL034210, 2008. 31168

Fuentes, E., Coe, H., Green, D., de Leeuw, G., and McFiggans, G.: Laboratory-generated primary marine aerosol via bubble-bursting and atomization, Atmos. Meas. Tech., 3, 141–162, doi:10.5194/amt-3-141-2010, 2010a. 31159, 31167

Fuentes, E., Coe, H., Green, D., de Leeuw, G., and McFiggans, G.: On the impacts of phytoplankton-derived organic matter on the properties of the primary marine aerosol – Part 1: Source fluxes, Atmos. Chem. Phys., 10, 9295–9317, doi:10.5194/acp-10-9295-2010, 2010b. 31168

Hodal, H., Falk-Petersen, S., Hop, H., Kristiansen, S., and Reigstad, M.: Spring bloom dynamics in Kongsfjorden, Svalbard: nutrients, phytoplankton, protozoans and primary production, Polar Biol., 35, 191–203, doi:10.1007/s00300-011-1053-7, 2012. 31156, 31157, 31168

Hop, H., Pearson, T., Hegseth, E., Kovacs, K., Wiencke, C., Kwasniewski, S., Eiane, K., Mehlum, F., Gulliksen, B., Wlodarska-Kowalezuk, M., Lydersen, C., Weslawski, J., Cochrane, S., Gabrielsen, G., Leakey, R., Lonne, O., Zajaczkowski, M., Falk-Petersen, S., Kendall, M., Wangberg, S., Bischof, K., Voronkov, A., Kovaltchouk, N., Wiktor, J., Poltermann, M., di Prisco, G., Papucci, C., and Gerland, S.: The marine ecosystem of Kongsfjorden, Svalbard, Polar Res., 21, 167–208, doi:10.1111/j.1751-8369.2002.tb00073.x, 2002. 31157, 31158, 31168

Hop, H., Falk-Petersen, S., Svendsen, H., Kwasniewski, S., Pavlov, V., Pavlova, O., and Søreide, J. E.: Physical and biological characteristics of the pelagic system across Fram Strait to Kongsfjorden, Prog. Oceanogr., 71, 182–231, doi:10.1016/j.pocean.2006.09.007, 2006. 31157, 31158

Hultin, K. A. H., Nilsson, E. D., Krejci, R., Mårtensson, E. M., Ehn, M., Hagström, Å., and de Leeuw, G.: In situ laboratory sea spray production during the Marine Aerosol Production 2006 cruise on the northeastern Atlantic Ocean, J. Geophys. Res.-Atmos., 115, D06201, doi:10.1029/2009JD012522, 2010. 31155, 31159

ACPD
12, 31153–31186, 2012

Hultin, K. A. H., Krejci, R., Pinhassi, J., Gomez-Consarnau, L., Mårtensson, E. M., Hagström, Å., and Nilsson, E. D.: Aerosol and bacterial emissions from Baltic Seawater, Atmos. Res., 99, 1–14, doi:10.1016/j.atmosres.2010.08.018, 2011. 31155, 31169

Ito, H. and Kudoh, S.: Characteristics of Water in Kongsfjorden, Proc. NIPR Symp. Polar Meteorol. Glaciol., 11, 211–232, 1997. 31158

Johannessen, O. M., Shalina, E. V., and Miles, M. W.: Satellite evidence for an Arctic sea ice cover in transformation, Science, 286, 1937–1939, doi:10.1126/science.286.5446.1937, 1999. 31155

Mårtensson, E. M., Nilsson, E. D., de Leeuw, G., Cohen, L. H., and Hansson, H.-C.: Laboratory simulations and parameterization of the primary marine aerosol production, J. Geophys. Res.-Atmos., 108, 4297, doi:10.1029/2002JD002263, 2003. 31155, 31169

Modini, R. L., Ristovski, Z. D., Johnson, G. R., He, C., Surawski, N., Morawska, L., Suni, T., and Kulmala, M.: New particle formation and growth at a remote, sub-tropical coastal location, Atmos. Chem. Phys., 9, 7607–7621, doi:10.5194/acp-9-7607-2009, 2009. 31170

Nuth, C., Moholdt, G., Kohler, J., Hagen, J. O., and Kääb, A.: Svalbard glacier elevation changes and contribution to sea level rise, J. Geophys. Res.-Earth, 115, F01008, doi:10.1029/2008JF001223, 2010. 31155

O'Dowd, C. D., Facchini, M. C., Cavalli, F., Ceburnis, D., Mircea, M., Decesari, S., Fuzzi, S., Yoon, Y. J., and Putaud, J.-P.: Biogenically driven organic contribution to marine aerosol, Nature, 431, 676–680, doi:10.1038/nature02959, 2004. 31168

Parkinson, C. L. and Cavalieri, D. J.: Arctic sea ice variability and trends, 1979-2006, J. Geophys. Res.-Oceans, 113, C07003, doi:10.1029/2007JC004558, 2008. 31155

Piehl Harms, A. A., Tverberg, V., and Svendsen, H.: Physical qualification and quantification of the water masses in the Kongsfjorden-Krossfjorden system cross section, in: Proceedings Paper, Oceans 07 IEEE Aberdeen, 061215-086, doi:10.1109/OCEANSE.2007.4302332, 2007. 31158

Polyakov, I., Timokhov, L., Dmitrenko, I., Ivanov, V., Simmons, H., Beszczynska-Möller, A., Dickson, R., Fahrbach, E., Fortier, L., Gascard, J.-C., Hölemann, J., Holliday, N. P., Hansen, E., Mauritzen, C., Piechura, J., Pickart, R., Schauer, U., Steele, M., and Walczowski, W.: Observational program tracks Arctic Ocean transition to a warmer state, EOS T. Am. Geophys. Un., 88, 398–399, doi:10.1029/2007EO400002, 2007. 31155

Russell, L. M. and Singh, E. G.: Submicron salt particle production in bubble bursting, Aerosol Sci. Tech., 40, 664–671, doi:10.1080/02786820600793951, 2006. 31155

ACPD
12, 31153–31186, 2012

Steele, M., Ermold, W., and Zhang, J.: Arctic Ocean surface warming trends over the past 100 years, Geophys. Res. Lett., 35, L02614, doi:10.1029/2007GL031651, 2008. 31155

Svendsen, H., Beszczynska-Möller, A., Hagen, J. O., Lefauconnier, B., Tverberg, V., Gerland, S., Ørbøk, J. B., Bischof, K., Papucci, C., Zajaczkowski, M., Azzolini, R., Bruland, O., Wiencke, C., Winther, J.-G., and Dallmann, W.: The physical environment of Kongsfjorden-Krossfjorden, an Arctic fjord system in Svalbard, Polar Res., 21, 133–166, doi:10.1111/j.1751-8369.2002.tb00072.x, 2002. 31157, 31158, 31168

Tremblay, J.-E., Bélanger, S., Barber, D. G., Asplin, M., Martin, J., Darnis, G., Fortier, L., Gratton, Y., Link, H., Archambault, P., Sallon, A., Michel, C., Williams, W. J., Philippe, B., and Gosselin, M.: Climate forcing multiplies biological productivity in the coastal Arctic Ocean, Geophys. Res. Lett., 38, L18604, doi:10.1029/2011GL048825, 2011. 31155

Tyree, C. A., Hellion, V. M., Alexandrova, O. A., and Allen, J. O.: Foam droplets generated from natural and artificial seawaters, J. Geophys. Res.-Atmos., 112, D12204, doi:10.1029/2006JD007729, 2007. 31155

Vaattovaara, P., Huttunen, P. E., Yoon, Y. J., Joutsensaari, J., Lehtinen, K. E. J., O'Dowd, C. D., and Laaksonen, A.: The composition of nucleation and Aitken modes particles during coastal nucleation events: evidence for marine secondary organic contribution, Atmos. Chem. Phys., 6, 4601–4616, doi:10.5194/acp-6-4601-2006, 2006. 31170

Zábori, J., Krejci, R., Ekman, A. M. L., Mårtensson, E. M., Ström, J., de Leeuw, G., and Nilsson, E. D.: Wintertime Arctic Ocean sea water properties and primary marine aerosol concentrations, Atmos. Chem. Phys., 12, 10405–10421, doi:10.5194/acp-12-10405-2012, 2012. 31155, 31156, 31162, 31171

Zhang, J.: Warming of the arctic ice-ocean system is faster than the global average since the 1960s, Geophys. Res. Lett., 32, L19602, doi:10.1029/2005GL024216, 2005. 31155

ACPD
12, 31153–31186, 2012

Table 1. Meteorological average conditions, ± standard deviations and minimum and maximum conditions during the water sampling period in summer (24 August to 7 September, 2009) and winter (15 February to 7 March, 2010). The values were measured in Ny-Ålesund and provided by the Norwegian Meteorological Institute.

	summer	winter
avg. air temperature (°C)	3.2 ± 1.7	−14.4 ± 4.1
max. air temperature (°C)	8.2	−1.7
min. air temperature (°C)	−0.9	−23.1
sum of precipitation (mm)	3.5	21.5
avg. air pressure (hPa)	1008.9 ± 11.4	1015.9 ± 13.9
max. air pressure (hPa)	1022.0	1032.8
min. air pressure (hPa)	993.6	967.4
avg. wind direction (°)	137.7 ± 94.2	156.0 ± 54.2
avg. wind speed ($m\,s^{-1}$)	1.5 ± 1.6	3.7 ± 3.6
max. wind speed ($m\,s^{-1}$)	7.4	19.9
min. wind speed ($m\,s^{-1}$)	0	0
avg. cloud cover (octas)	5.4 ± 2.9	2.8 ± 3.0
max. cloud cover (octas)	8	8
min. cloud cover (octas)	0	0

ACPD
12, 31153–31186, 2012

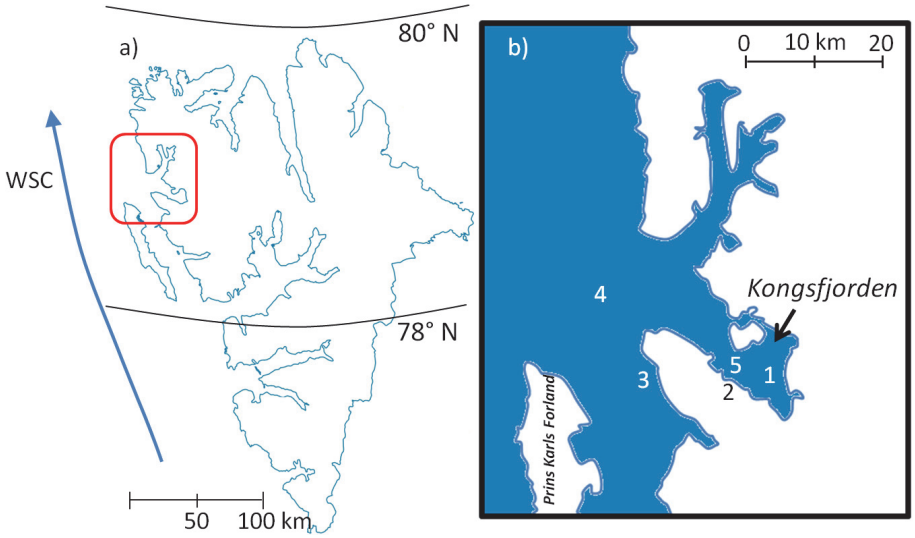

Fig. 1. (a) Overview map of the investigation area (marked red). Blue arrow indicates the direction of the West Spitsbergen Current (WSC). **(b)** Sampling locations. Point 1: close to the glacier (summer and winter measurements); point 2: marine laboratory with deep sea water inlet in Ny-Ålesund (summer and winter measurements); point 3: outside of Kongsfjorden (winter measurements); point 4: outside of Kongsfjorden (summer measurements); point 5: middle of the fjord (summer measurements).

ACPD
12, 31153–31186, 2012

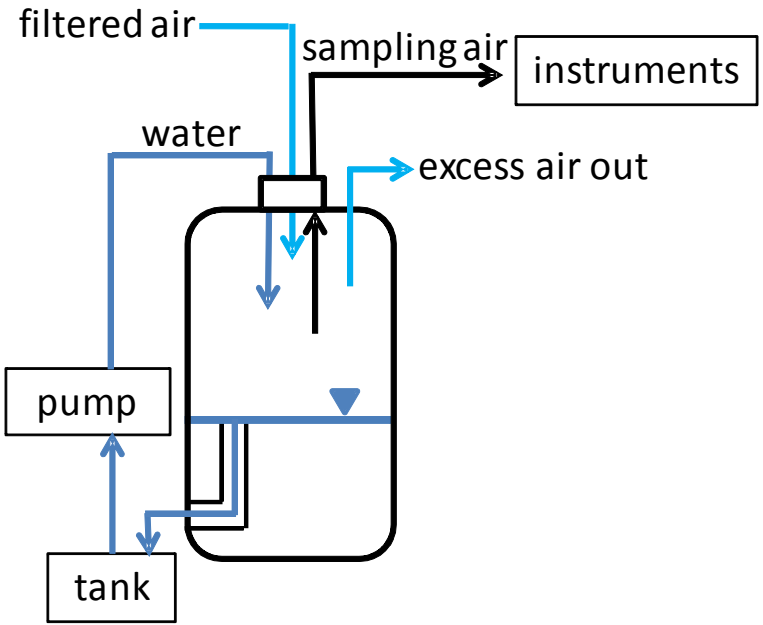

Fig. 2. A schematic picture of the bubble bursting experimental setup. The tank was used as a buffer to recirculate the sea water sample trough the PET bottle, where sea spray aerosols were produced by an impinging water jet. Darker blue lines represent water, and the triangle symbol indicates the water surface in the bottle.

ACPD
12, 31153–31186, 2012

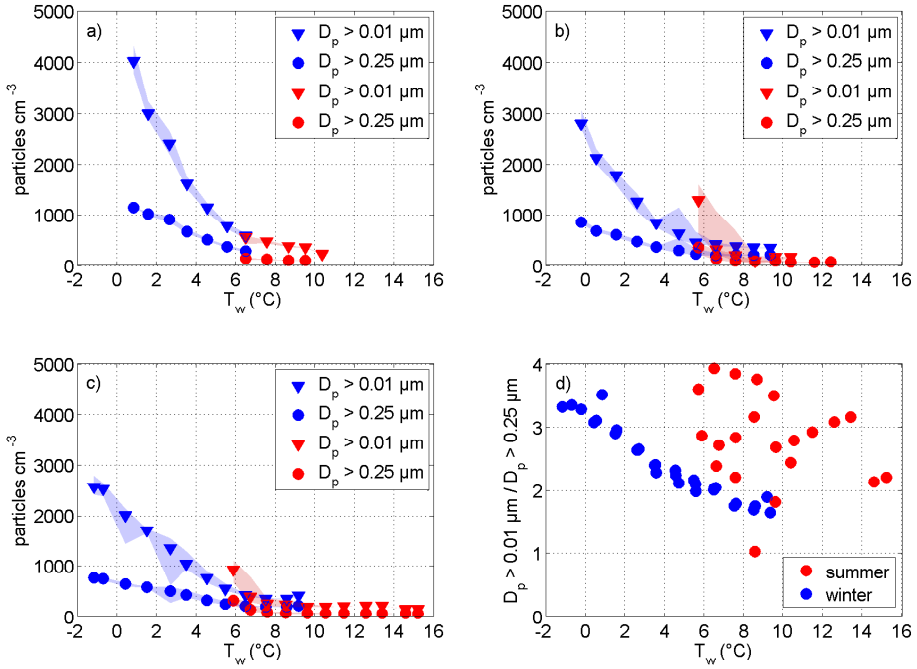

Fig. 3. The median particle number concentrations as a function of water temperature (T_w). Blue data points represent winter data and red data points summer data with triangles for particles $D_p > 0.01\,\mu m$ and circles for particles with $D_p > 0.25\,\mu m$. Blue and red shaded areas represent the interquartile ranges. Particle number concentrations resulted from bubble bursting in **(a)** deep fjord water **(b)** water sampled close to glacier **(c)** water sampled at the fjord mouth **(d)** ratio between particle number concentration of particles $D_p > 0.01\,\mu m$ and $D_p > 0.25\,\mu m$. The ratios were built for each data point pair shown in **(a–c)**.

ACPD
12, 31153–31186, 2012

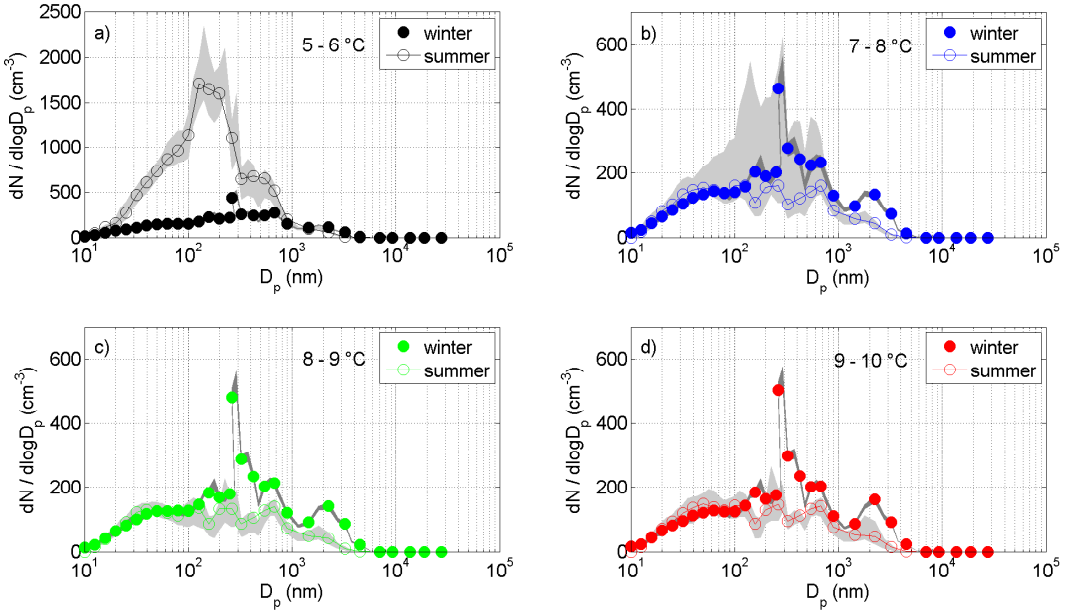

Fig. 4. Comparison of particle number size distributions resulting from water sampled close to the glacier during summertime and wintertime, for the same water temperature ranges of **(a)** 5–6 °C **(b)** 7–8 °C **(c)** 8–9 °C **(d)** 9–10 °C. For clarity reasons only every second data point is shown. Grey shaded areas represent the interquartile ranges. Note the different scale for the lowest temperature range.

ACPD
12, 31153–31186, 2012

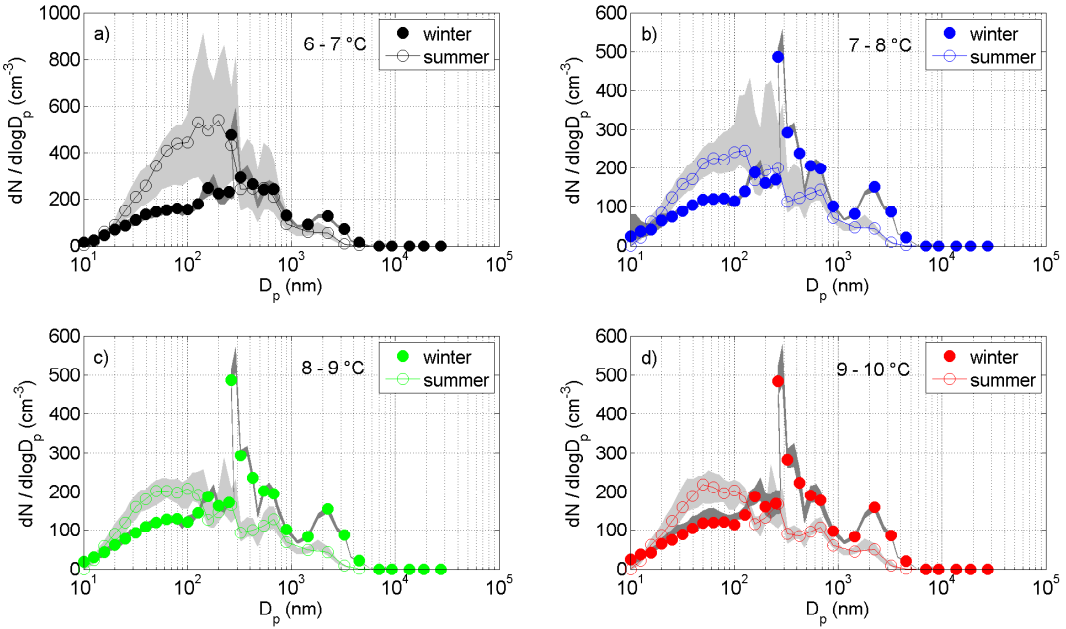

Fig. 5. Comparison of particle number size distributions resulting from water sampled close to the fjord mouth during summertime and wintertime, for the same water temperature ranges of **(a)** 6–7 °C **(b)** 7–8 °C **(c)** 8–9 °C **(d)** 9–10 °C. For clarity reasons only every second data point is shown. Grey shaded areas represent the interquartile ranges. Note the different scale for the lowest temperature range.

ACPD
12, 31153–31186, 2012

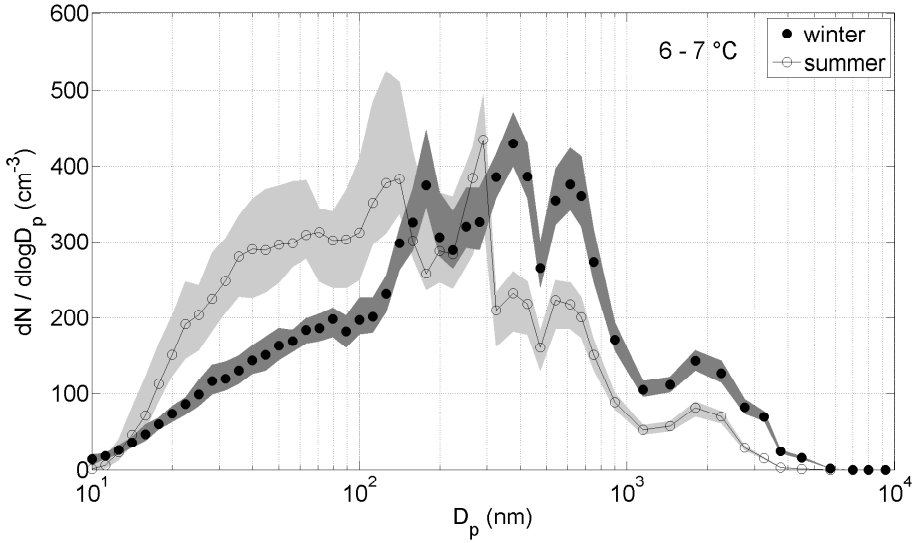

Fig. 6. Comparison of particle number size distributions resulting from deep sea water during summertime and wintertime, for the same water temperature ranges of 6–7 °C. Grey shaded areas represent the interquartile ranges.

ACPD
12, 31153–31186, 2012

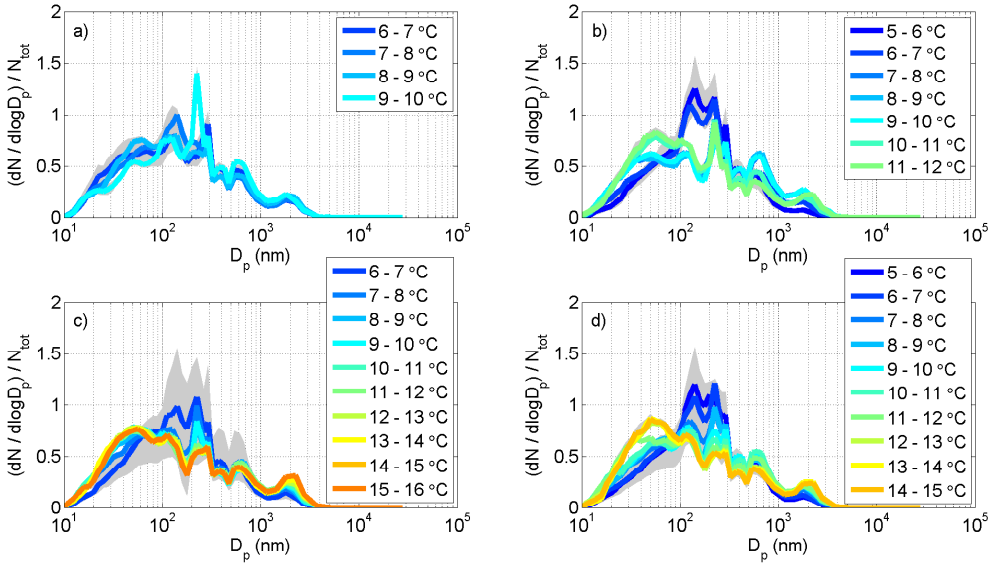

Fig. 7. Normalized number size distributions for summer experiments resulting from bubble bursting of **(a)** deep fjord water **(b)** water sampled close to the glacier **(c)** water sampled at the fjord mouth **(d)** water sampled at the middle of the fjord. Grey shaded areas represent the interquartile range for the lowest and highest water temperature range. The same grey shade is used for both temperature ranges and indicates if there is an obvious difference between the particle number concentrations of different sizes of the lowest and highest water temperature.

ACPD
12, 31153–31186, 2012

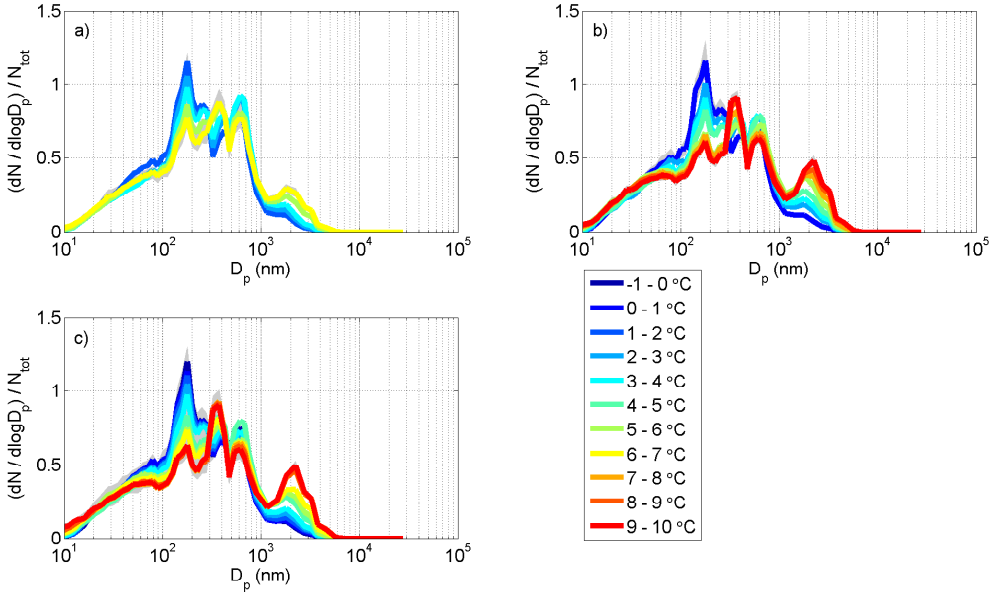

Fig. 8. Normalized number size distributions for winter experiments resulting from bubble bursting of **(a)** deep fjord water **(b)** water sampled close to the glacier **(c)** water sampled at the fjord mouth. Grey shaded areas represent the interquartile range for the lowest and highest water temperature range. The same grey shade is used for both temperature ranges and indicates if there is an obvious difference between the particle number concentrations of different sizes of the lowest and highest water temperature.

ACPD
12, 31153–31186, 2012

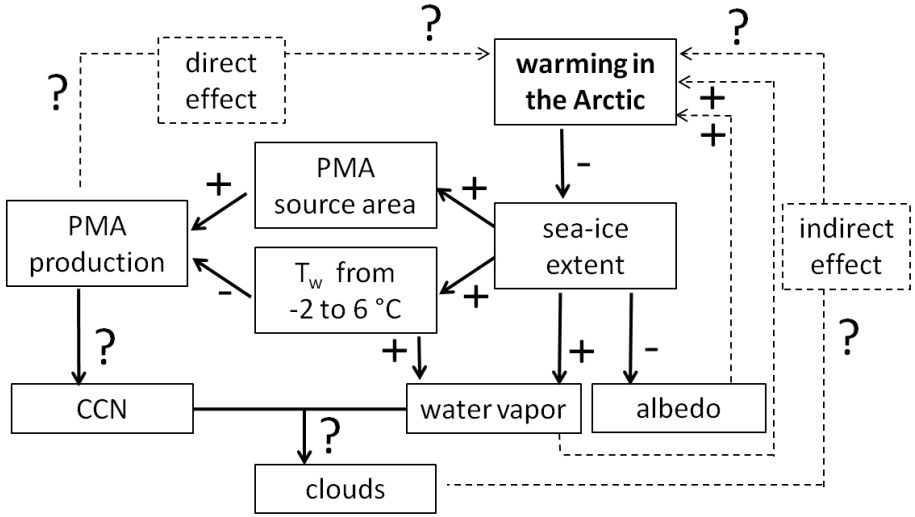

Fig. 9. Potential feedback loop resulting from a warming in the Arctic. Plus signs indicate increases and minus signs indicate decreases. Question marks indicate that the direction of the change is not clear.

ACPD
12, 31153–31186, 2012